

## TIME AS A GAUGE FIELD

**Arturo Tozzi**, MD, PhD, AAP (Corresponding Author)  
Center for Nonlinear Science, University of North Texas, Denton, Texas 76203, USA  
tozziarturo@libero.it

**James F. Peters**, Dr., Professor  
Department of Electrical and Computer Engineering, University of Manitoba  
75A Chancellor's Circle  
Winnipeg, MB R3T 5V6 CANADA  
James.Peters3@umanitoba.ca

**Clifford Chafin**  
Roto9 Energy, Chapel Hill, NC, USA  
cliff.chafin@gmail.com

**Domenico De Falco**, AP  
Second University of Naples, Dipartimento di Ingegneria Industriale e dell'Informazione, Aversa, Caserta, Italy  
domenico.defalco@gmail.com

The concepts of “constraints” and “virtual displacement” from analytical mechanics shed new light on the role of time and timescales in physical systems such as the Universe. We propose a covariant version of a gauge theory, in which the required global symmetry stands for the real constrained trajectories, i.e. the energetic gradient flows dictated by the second law of thermodynamics. The virtual displacements, occurring while time is held constant, stand for the local transformations acting on the system and able to “break” the symmetry. The time stands for the gauge field able to keep the Lagrangian invariant. We also provide a theoretical framework in which a topological approach to gravitational lenses is able to elucidate aspects of our theory of “time as a gauge field”. Thus, time is no longer one of the four phase space coordinates of a 4-D Riemannian Universe: it is just a gauge field superimposed to a 3-D system.

**KEY WORDS:** time, gauge theory, symmetries, constraints, informational entropy

## INTRODUCTION

Many current theories emphasize the foremost role of the “time” and “timescales” in different physical and biological fields, from cosmology – the 4-D Riemannian Universe –, to cellular function<sup>1</sup> and neural activity<sup>2,3</sup>. Is such a tenet true? Although stochastic variables and random fluctuations regulated by the Langevin and the Fokker-Planck equations frequently occur<sup>4</sup>, physical and biological activities are only partially Brownian, since they are “constrained”. For example, the protein-folding final conformation is dictated by the minimum frustration principle on long evolutionary timescales, which states that proteins’ energy decreases more than expected, as they assume conformations progressively more like the native state<sup>5,6</sup>. A strong bias in the protein’s surface energy landscape towards the native basin occurs, overcoming the asperities of the rugged landscape<sup>7,8</sup>. In other words, proteins were enriched by evolution for sequences with the propensity to fold into the lowest energetic structures. Constraints also occur in countless other systems, from the nonlinear chaotic paths governed by strange attractors, to the structure of biological entities, ruled by their specific genetic pools. Despite the large number of different scenarios, the processes governing constraints on physical and biological systems may be generalized, taking into account a universal principle: the second law of thermodynamics, which states that “*every process occurring in nature proceeds in the sense in which the sum of the entropies of all bodies taking part in the process is increased*” (Planck’s formulation). In such a framework, the concepts of “virtual displacement” - from the far-flung branch of analytical mechanics - come into play<sup>9,10,11,12</sup>. In this paper we will indeed elucidate, via a gauge theory, that close relationships occur among virtual displacements, probabilities and time. In order to assess our theory, we also use the concept of gravitational lens. The latter is a distribution of matter (such as a cluster of galaxies) between a distant source and a terrestrial observer, capable of bending the light from the source, as it travels towards the observer. The amount of bending is one of the predictions of Einstein’s general theory of relativity. For example, the light from a distant galaxy is deviated due to the gravitational effects of a foreground celestial body, which acts like a lens and makes the distant source appear either distorted and magnified. In this paper, we argue that the

mechanism of gravitational lenses can be explained in the algebraic topological terms of the Borsuk-Ulam theorem. Such a finding makes it possible to hypothesize a theory of time as a gauge field. The manuscript contains four sections. The first section describes the virtual and real constraints in the framework of a “frozen” time. The second section, taking into account probabilistic arguments, shows how is possible to insert virtual constraints on the Shannon entropy’s plot, in order to correlate informational entropy with the arrow of time. The third section illustrates the procedure to sketch gauge theory based on the three above mentioned ingredients: constraints, probabilities and time. In the fourth section, a topological approach to gravitational lenses comes into play and shows how the methodology can be applied in order to clarify a theory of “time as a gauge field”.

## VIRTUAL CONSTRAINTS

The key concept of virtual constraints is a dynamically imposed outer feedback control, so that the trajectory of a particle or an agent in the system’s phase space can be “forced” towards the desired orbits and outputs<sup>13</sup>. The virtual constraints reduce the degrees of freedom, coordinating the evolution of the various links throughout a single variable. A closed-loop mechanism is achieved, wherein dynamic behaviour is fully determined by the evolution of simplest lower-dimension system<sup>14</sup>. The resulting system is called a “virtual limit system”.

In mathematical terms, we define a set of  $n - 1$  outputs (or constraints):

$$y = \varphi(p, q) = \bar{q} - h(\theta, p) = \bar{q} - h(\theta, p(t)),$$

where  $y$  and  $\varphi(p, q)$  are the outputs or constraints,  $\bar{q} \in R^{n-1}$  is a vector describing the actuated coordinates and velocities,  $p$  is the set of the design parameters,  $\theta \in R$  is the unactuated variable,  $\theta(q)$  is a function of the generalized coordinates of  $q$ . The latter equation describes the most general condition.

An inner-feedback loop is used to perform output feedback linearization in a local domain, where the matrix is invertible:

$$\psi(q)u = k(q; \dot{q}) + v,$$

where  $v$  is the outer feedback loop. Note that the equation includes a term  $\dot{q}$  which depends on time, where the upper

dot stands for the partial time derivative, i.e.,  $\dot{q} = \frac{\partial q}{\partial t}$  (de Wit *et al.* 2003)<sup>26</sup>.

If an outer feedback loop  $v$  is designed to zeroing the output  $y$ , we get a partially linearized system in the form:

$$\ddot{y} = v.$$

Then the full system dynamic is captured by the solutions of:

$$\alpha(\theta)\ddot{\theta} + \beta(\theta)\dot{\theta}^2 + \gamma(\theta) = 0,$$

together with the imposed constraint for mean  $q$ -value:

$$\bar{q} = h(\theta, p),$$

where  $\theta(q)$ ,  $\alpha(\theta)$ ,  $\beta(\theta)$  and  $\gamma(\theta)$  are scalar functions depending on the inner feedback loop.

In conclusion, the virtual constraints are forces external to the system’s phase space, able to modify an internal trajectory towards the required one. This process allows one to deal with high-dimensional systems with underactuated degree one, by only analyzing this second-order nonlinear equation.

In analytical mechanics the researchers cope with under-actuated Lagrangian systems of the form:

$$\frac{d}{dt} \left( \frac{\partial L}{\partial \dot{q}} \right) - \frac{\partial L}{\partial q} = B(q)u,$$

where  $q$  and  $\dot{q}$  are vectors of generalized coordinates and velocities,  $L(q; \dot{q})$  is a Lagrangian of the system,  $B(q)$  is a matrix function of an appropriate dimension, with rank equal to the number of inputs and  $u$  is a vector of independent control inputs. The under-actuation means that  $\dim u < \dim q$ , i.e., the number of actuators is less than the number of its degrees of freedom.

A virtual displacement is an assumed change of system coordinates occurring while time is held constant. It is called “virtual” rather than “real”, since no actual displacement takes place without the passage of time. Computerized simulations may be performed to see what happens to physical and biological paths when time is kept fixed, *e.g.*, during the movements of animals in an environment, or during cytoplasmatic enzymatic reactions. For further details about the methodology, see **Figure 1**.

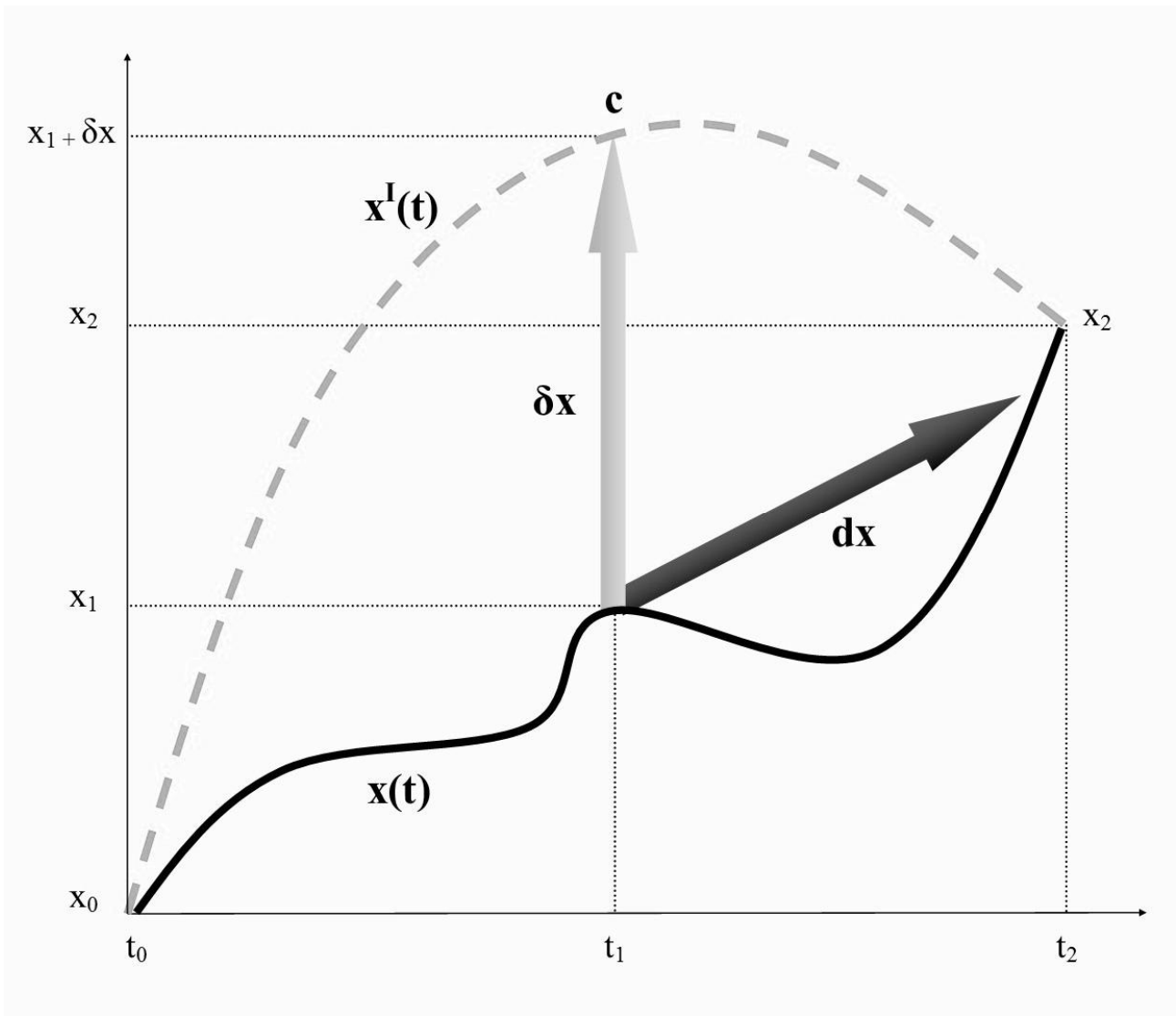


**Figure 1.** A graph plotting time  $t$  on the X-axis and the space  $x$  on the Y-axis. We evaluated two trajectories which both display a starting position at  $x_0$  and an ending position at  $x_2$ . The black solid curve  $x(t)$  is the particle trajectory, while the dotted black curve  $x^I(t)$  is the virtual trajectory. At position  $x_1$  and time  $t_1$ , the virtual displacement  $\delta x$  - from  $x_1$  to the point  $c$  - is shown (grey arrow). The regular displacement  $dx$  is a vector pointing in the direction of the motion (black arrow), which arises from differentiating with respect to time parameter along the path of the motion. In contrast, the virtual displacement  $\delta x$  is a tangent vector to the constraining manifold at a fixed time, because it arises from the differentiation with respect to the enumerating paths of the motion, varied in a manner consistent with the constraints.

## INFORMATIONAL ENTROPY AND TIME

The real displacements are governed by the second law of thermodynamics. In every system, either physical or biological, the thermodynamical entropy relentlessly increases from time  $T_0$  to  $T_2 = \infty$ , until its maximum value. In our case, it is however preferable to use the informational entropy, instead of the thermodynamical one. Indeed, the two entropies are linked through the formula:

$$S = k H$$

in which  $S$  is the thermodynamical entropy,  $k$  is the Boltzmann constant and  $H$  is the Shannon informational entropy. The informational entropy, apart from the invaluable advantage of quantifying the macroscopic states without a perfect knowledge of the microscopic ones, is not directly linked with time, allowing us to remove such parameter from our system. However, we need to introduce the arrow of time on the "classic" Shannon's curve: we did it by adding a third dimension to its 2-D plot (**Figure 2**). The vector of time  $\zeta$  lies in a plane forming an angle  $A$  with the 2-D plane of

Shannon entropy. Note that the timescales expressed by the vector  $\zeta$  in the graphic may vary, depending on which system we are evaluating. As an example, if we take into account the system Universe,  $T_0$  stands for the state of minimum entropy – the initial Big Bang -, while  $T_2 = \infty$  stands for the state of maximum entropy, *i.e.*, the hypothetical final state of the Universe. Starting from the probability of a virtual constraint  $c$ , we may calculate the corresponding point  $T_1$  on the arrow of time, in order to know how much time is still required to reach  $T_2 = \infty$  (which stands for the system’s “real” final state at the energetic equilibrium). There is however a still unknown parameter left: the value of the angle  $A$ , which is not implied to be constant, but could change in different examined systems. The next section answers the question: how can we find the value of the angle  $A$ ?

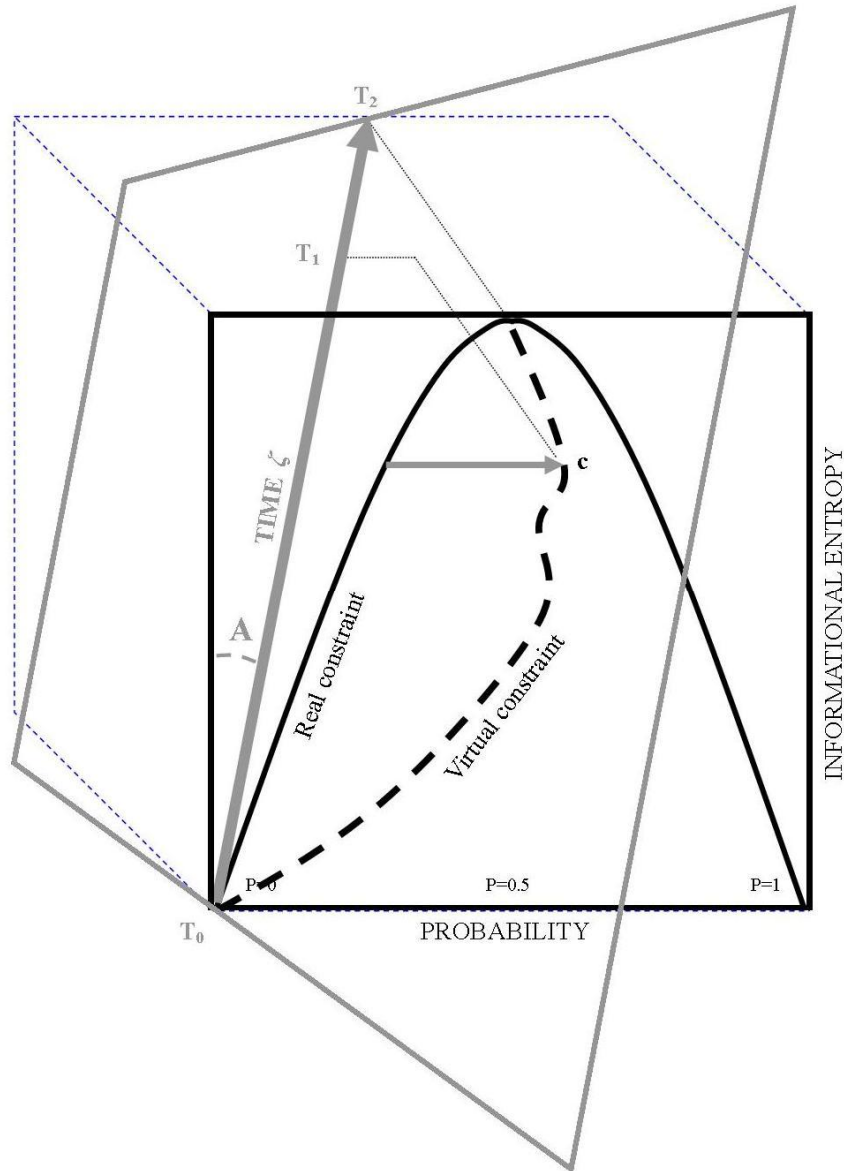


**Figure 2.** The informational entropy is plotted as a function of the random variable  $p$ , in the case of two possibilities with probabilities  $p$  and  $(1-p)$ . The solid line black stands for the Shannon entropy (under ergodic conditions). The values  $p=0$  and  $p=1$  stand for the minimum entropy,  $p=0.5$  for the maximum entropy. The arrow of time  $\zeta$  (grey solid line) lies on a third coordinate of the phase space and is equipped with the angle  $A$ . Due to the energetic gradient flows dictated by the second law of thermodynamics, the time, in its route from  $T_0$  to  $T_2 = \infty$ , is correlated with an increase in informational entropy. Given a virtual displacement  $c$  on the virtual trajectory (dotted black line), the corresponding value of  $T_1$  on the arrow of time can be calculated, provided the value of  $A$  is known.

## TIME IS A GAUGE FIELD: BUILDING A GAUGE THEORY

Here we examine the possibility to sketch a on differential geometry-based theory of the real and virtual trajectories' phase space. We need to build a system where the real displacement - the real trajectory of particles or events - stands for the continuous, global symmetry. Such a symmetry consists in the energetic constraints that the second law of thermodynamics enforces on the system. However, the energetic gradient flow occurs just in long timescales. In turn, in the very instant in which  $T$  is "frozen", fixed and equals to zero, the virtual displacement occurs, standing for a continuous group of local transformations able to "break" the symmetry. The local loss of symmetry (a disturbance of the gradient flow) needs however to be ripristinated, by introducing a continuous field - the time - able to restore the gradient flow. The time, in such a framework, stands for a field acting on the system, which is continuous at nonrelativistic timescales. There are many possible ways to deal with a theory of the virtual displacements in a differential geometric sense, for example by analyzing them in terms of sections of fibre bundles, jet manifolds and Ehresmann connections<sup>15,16,17</sup>. We went through a system characterized by a global invariant symmetry. In order to quantitatively assess the required forces, we followed the procedure shown in the oversimplified **Figure 3**. In **Figure 3A**, as an example, we choose four random areas in a 3D system and equipped them with transformations belonging to the  $SO(2)$  Lie group, isomorphic to the rotation group of the circle. The Lie group stands for the measure of probability density in each of the four areas. The manifold is unfolded and flattened into a two-dimensional reconstruction<sup>18</sup> (**Figure 3B**), allowing the entire system surface to be transferred to an atlas  $M$  of  $C^\infty$  (smooth), finite dimensional manifolds, each corresponding to one of the four single areas at a fixed time= $0$  (**Figure 3B**). The set of virtual displacements describing area-specific probabilities stands for a continuous group of local transformations acting on sections of  $M$ .  $M$  is thus equipped with a constant matrix  $G$  belonging to the  $SO(2)$  Lie group.

$M$  is a principal  $G$ -bundle  $P$  characterized by a trivial, smooth and differentiable fibre bundle, by vector bundles  $E$  and by a tangent bundle  $TE$  (**Figure 3B**). Virtual displacements are described by a field of vectors and angles, representing the action  $G$  on the chosen local section  $E$  of  $P$ . **Figure 3B** depicts the four forces  $G$  as four vector bundles  $E$  arising from four points  $p$  in the tangent space  $T_p$ . They are equipped with four  $n$ -dimensional rotation angles  $\varphi$  ( $\varphi_1, \varphi_2, \dots, \varphi_n$ )<sup>T</sup> representing the (local) virtual displacement (expressed in terms of probability state) of every area. Rotations through tiny angles link nearby transformations of angles  $\varphi$  arising from points  $p$ : as a result, the linear approximation of the function  $G$  at  $p$  (and its angle  $\varphi$ ) in each dimension can be described by introducing a partial derivative. Changes in degree of  $\varphi$  in selected areas match with virtual displacements' different probabilities and hence with different trajectory configurations.

The geometric "link" between  $L$  and  $\varphi$  can be defined in terms of a connection form, the Ehresmann connection<sup>19</sup>. If we identify the horizontal space  $H$ , perpendicular to the vertical space  $VE$ , we can extrapolate the Ehresmann connection  $\omega$ , which is a vector on  $TE$  (**Figure 3B**). The Lagrangian density  $L$  is indeed a function of  $TE$  and  $H$ . It is possible to formulate all rates of change of  $\omega$  and  $\varphi$  in terms of a covariant derivative - a linear differential operator in each associated  $TE$  - which allows different points (and their angles) to be compared. By mapping every vector  $\omega$  of  $P$  into the bijective, diffeomorphic  $P^l$  space, a curvature form is constructed (**Figure 3C**). When the vectors  $\omega^l$  intersect the unique horizontal lift corresponding to the invariant  $L$ , the angles  $\sigma$  are achieved. The behaviour of the vectors  $\omega^l$  and the angles  $\sigma$  can be described compactly by point-wise vector addition of the partial derivatives of the function  $G$  at each point. As a result, we get a single vector:  $\vec{\Omega} = \vec{\omega}_1 + \vec{\omega}_2 + \dots + \vec{\omega}_n$ . The angle  $\Sigma$  is introduced (**Figure 3D**), standing for the interaction Lagrangian  $L_{int}$  and expressing the values of vector addition.

If the lines  $L$  and  $\Omega$  are parallel,  $\Sigma$  equals zero,  $L_{int}$  equals  $L$  and the symmetry of the system is preserved. Otherwise, if  $L$  and  $\Omega$  are not parallel (as in nearly all physical and biological systems at  $T=0$ ),  $\Sigma$  is different from zero,  $L_{int}$  is different from  $L$  and the system displays a "broken" symmetry. In this case - to ensure the invariance of  $L$  and to restore the symmetry - we need to define a covariant derivative such that the derivative of  $\Sigma$  will again transform identically with  $\Sigma$ . According to the covariant version of gauge theories<sup>20</sup>, the correction terms are reinterpreted as couplings to an additional divergent counter term, the gauge field, by allowing the symmetry parameter to vary from place to place in the local coordinate system. **Figure 3E** shows the procedure in a very abridged form. If we do not take  $L$  into account and examine the sole vector  $\Omega$  and its angle  $\Sigma$ , we observe nothing else than a single force. If instead we regard  $L$  as a vector that results from the scalar components of its vector space  $v$ , then  $\Omega$  (and its angle  $\Sigma$ ) turns out to be just one of the covariant components of  $L$ . To ensure that  $L$  is invariant, we need to add another component: we introduce the vector  $\zeta$ , equipped with the angle  $\Pi$ . The latter stands for the gauge field Lagrangian  $L_{gf}$  and expresses the global value of the required gauge field. We are thus able to make accurate predictions of the forces: we can extrapolate from  $\Pi$  the values of the gauge field required to render the trajectories invariant under different virtual displacements.

Our scheme resembles a gauge theory<sup>21,22</sup>, but with some distinctions. The physical gauge theories are based on three tenets<sup>23,24</sup>:

- a) The system is equipped with a continuous, preserved "global" symmetry (and a corresponding Lagrangian).
- b) The system displays a continuous group of "local" transformations, equipped with a Lie group.

- c) The Lagrangian is kept invariant under such local transformations by a “gauge field”, i.e. a continuous force acting on the system.

The Lagrangian, through its connections with Noether’s theorem, throws a bridge between symmetries and energetic requirements. Note that the concept of the Lagrangian is slightly different in our model: instead of referring to the principle of least action and the “preservation” of a physical quantity as usual in gauge theories, it refers to the “dissipation” of a physical quantity through a gradient flow.

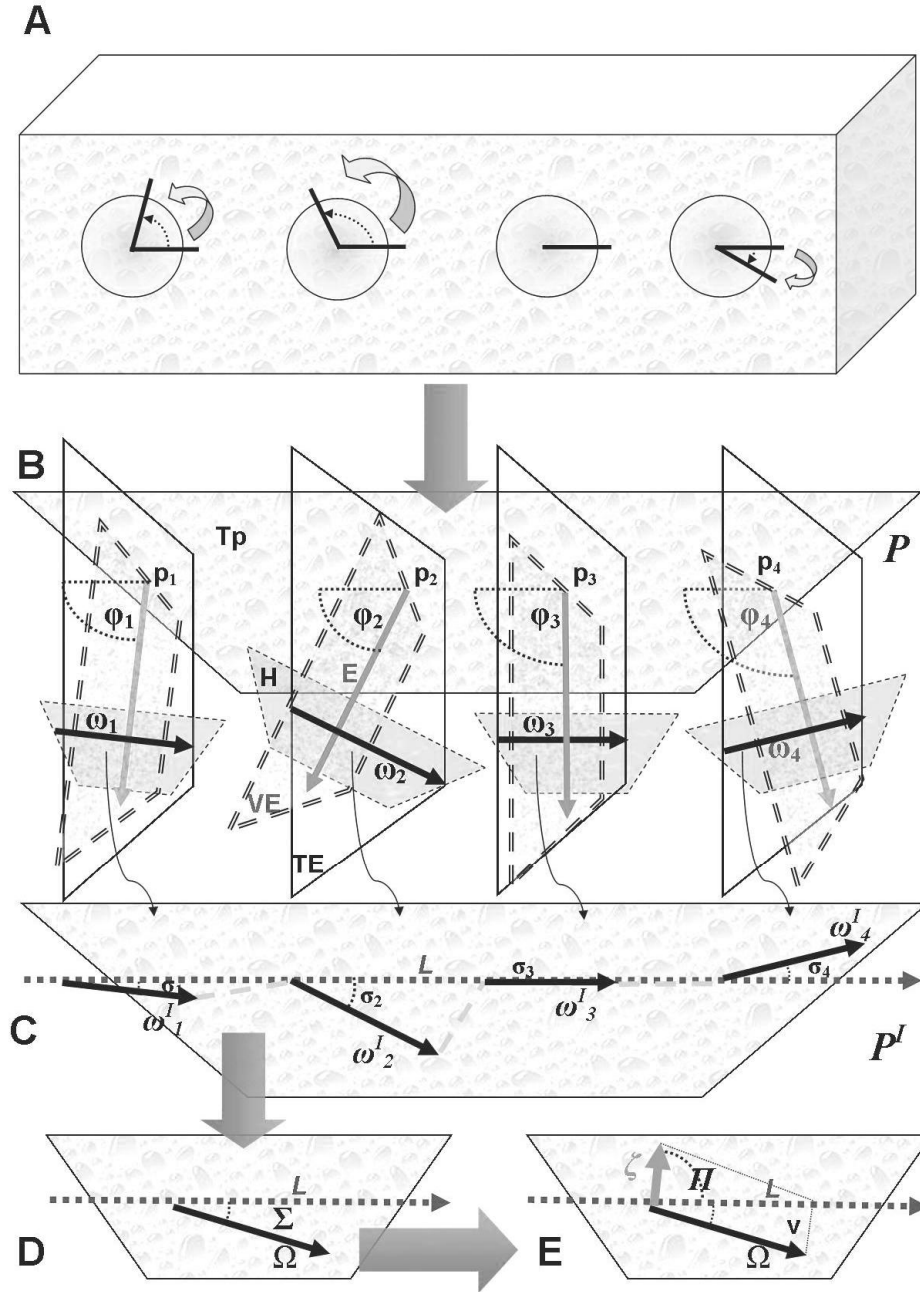


**Figure 3.** Oversimplified analysis of virtual displacements in a system equipped with a global, invariant symmetry (the real constraints). Four virtual displacements - expressed as measures of probability states in four areas of a 3D system, at time kept fixed at zero - are equipped with a Lie group (**Figure 3A**) and mapped on a 2-D manifold (**Figure 3B**). An Ehresmann connection is performed (**Figure 3C**) and the required gauge field (the vector  $\zeta$ , equipped with the angle  $\Pi$ ) can be calculated (**Figures 4D-E**). See the main text for further details.

## TIME AS A GAUGE FIELD: CLUES FROM A TOPOLOGICAL APPROACH TO GRAVITATIONAL LENSES

In this section we argue that the mechanism of gravitational lenses can be explained in the algebraic topological terms of the Borsuk-Ulam theorem (BUT). Indeed, gravitational lensing in the framework of BUT provides us the mathematical apparatus to build the theory of time as gauge field, which is otherwise too theoretical and untestable.

At first, we need to discuss the “standard” version of the Borsuk-Ulam theorem (BUT), which states states that (Borsuk)<sup>29,30</sup>:

*Every continuous map  $f : S^n \rightarrow R^n$  must identify a pair of antipodal points (on  $S^n$ ).*

This means that the  $n$ -sphere  $S^n$  maps to the space  $R^n$ , which is an  $n$ -dimensional Euclidean space. Another less technical definition is: if a sphere is mapped continuously into a plane set, there is at least one pair of antipodal points having the same image; that is, they are mapped to the same point of the plane (Dodson)<sup>31</sup>. The notation  $S^n$  denotes an  $n$ -sphere, which is a generalization of the circle. A  $n$ -sphere is a  $n$ -dimensional structure embedded in a  $n+1$  space. For example, a 1-sphere ( $S^1$ ) is the one-dimensional circumference surrounding a 2-dimensional disk, while a 2-sphere ( $S^2$ ) is the 2-dimensional surface of a 3-dimensional ball (a beach ball is a good example). An  $n$ -sphere is formed by points which are constant distance from the origin in  $(n+1)$ -dimensions. For example, a 3-sphere (also called *glome* or *hypersphere*) of radius  $r$  (where  $r$  may be any positive real number) is defined as the set of points in 4D Euclidean space at distance  $r$  from some fixed center point  $c$  (which may be any point in the 4D space). A 3-sphere is a simply connected 3-dimensional manifold of constant, positive curvature, which is enclosed in a Euclidean 4-dimensional space called a 4-ball. A 3-sphere is thus the surface or boundary of a 4-dimensional ball, while a 4-dimensional ball is the interior of a 3-sphere, in the same way as a bottle of water is made of a glass surface and a liquid content.

Points on  $S^n$  are *antipodal*, provided they are diametrically opposite. Examples of antipodal points are the endpoints of a line segment, or the opposite points along the circumference of a circle. Further, every continuous function from a  $n$ -sphere  $S^n$  into Euclidean  $n$ -space  $R^n$  maps some pair of antipodal points of  $S^n$  to the same point of  $R^n$ . For example, if we use the mapping  $f: S^3 \rightarrow R^3$ , then  $f(x)$  in  $R^3$  is just a signal value (a real number associated with  $x$  in  $S^3$ ) and  $f(x) = f(-x)$  in  $R^3$ . When  $g: S^2 \rightarrow R^2$ , the continuous function  $g(x)$  in  $R^2$  is a vector in  $R^2$  that describes the  $x$  embedded in  $S^2$ . In other words, a point embedded in a  $R^n$  manifold is projected to two opposite points on a  $S^{n+1}$ -sphere, and vice versa.

It is noteworthy that the concept of antipodal points can be generalized to countless types of system signals. The two opposite points can be used not just for the description of simple topological points, but also for more complicated structures, such as shapes of space (spatial patterns), shapes of time (temporal patterns), vectors or tensors, functions, signals, thermodynamical parameters, movements, trajectories, and general symmetries too (Peters)<sup>28</sup>. If we simply evaluate systems activity instead of “signals”, BUT leads naturally to the possibility of a region-based geometry (called ReBUT), instead of point-based one, with many applications. Indeed, a region can have features such as area, diameter, average signal value, and so on. The concept of reBUT and generalized antipodal points may be also applied to the mechanism of gravitational lenses (**Figure 4**). We are allowed to describe gravitational lenses’ regional features (i.e., average gradient direction, average intensity, feature vectors with many components, such as, for example, diameter, surface area, and gradient direction) as antipodal points on a  $n$ -sphere: the antipodal points, even if they are distorted, display indeed matching descriptions. A cosmic body emitting a light stands for the single point embedded in  $R^{n-1}$ , which projects to two antipodal points onto a  $n$ -sphere embedded in a dimension higher, i.e.,  $R^n$ . In other words, if we map the two opposite points on an  $n-1$  sphere, we obtain a single point, and vice versa. The two antipodal points standing for systems features are assessed at one level of observation, while the single point is assessed at a lower level. The BUT scenario provides, in this way, a vehicle for characterizing and modelling gravitational lenses.

It can be argued that the antipodal points on a gravitational lens are not exactly “opposite” each other. However, the applications of BUT can be generalized not just for the evaluation of brain symmetries as antipodal points, but also for non-antipodal points on an  $n$ -sphere (Peters)<sup>28</sup>. We can also consider homotopic regions on an  $n$ -sphere that are either adjacent or far apart. And BUT applies, provided there are a pair of regions on an  $n$ -sphere with the same feature values. We are thus allowed to say that the two points (or regions) do not need necessarily to be antipodal, in order to be described together (Peters)<sup>28</sup>. This makes it possible to evaluate matching signals, even if they are not “opposite”, but “near” one each other: the antipodal points restriction from the “classical” BUT is no longer needed.

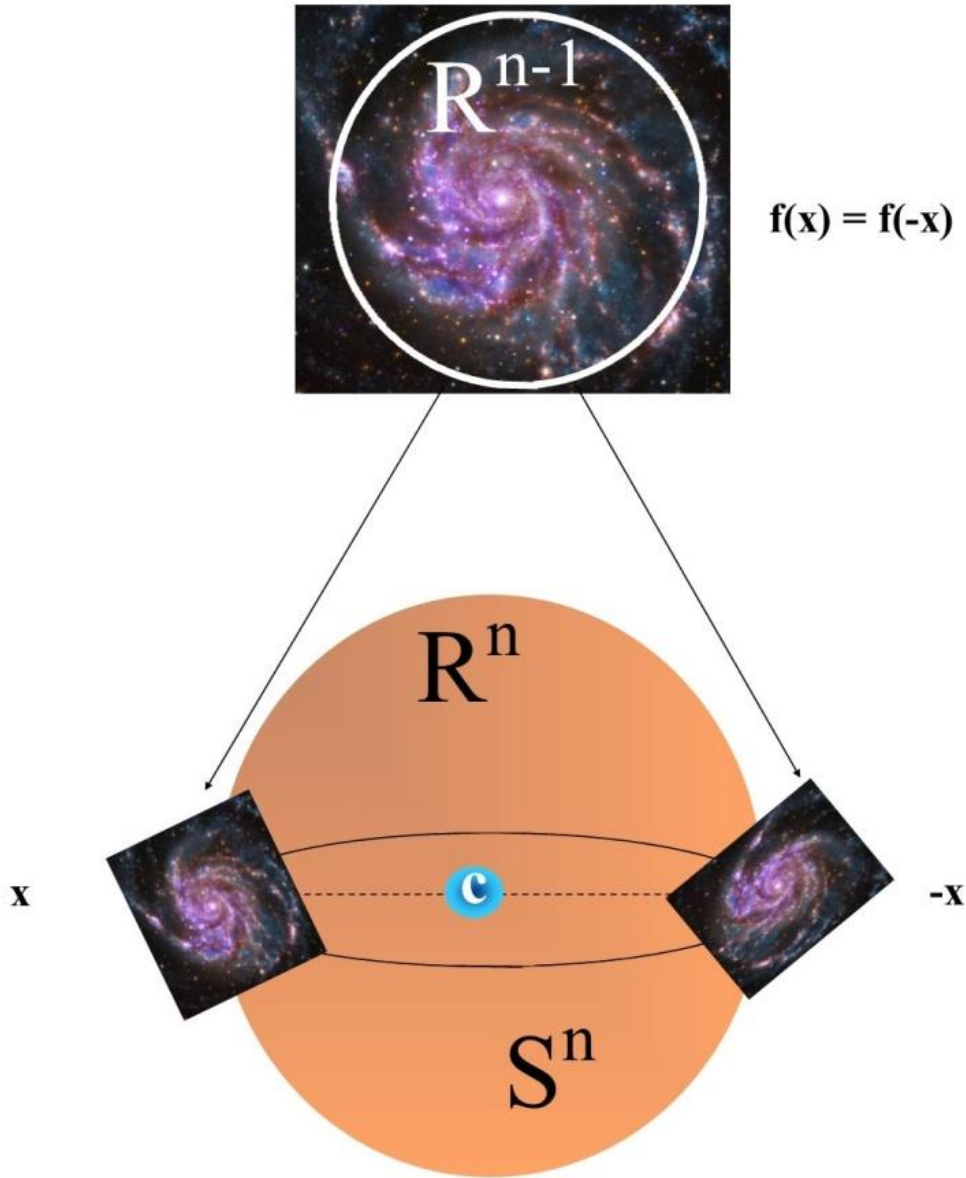


**Figure 4.** A simplified scheme of the application of the Borsuk-Ulam theorem to a gravitational lens. Two antipodal points in  $S^n$  project to a single point in  $R^n$ , and vice versa. Remind that every  $S^n$  is embedded in a  $n+1$ -ball, so that every  $S^n$  is one-dimension higher than the corresponding  $R^n$  manifold. See the main text for further details.

**A 3D Universe... plus time.** By applying the equations of general relativity, the measure of the curvature of gravitational lens makes it possible to calculate the mass of the hidden cosmic object. Indeed, according to general relativity, when light passes around a massive object, it is distorted and bent towards an observer's eye, because of the curvature of the 4D spacetime. Since light moves at a constant speed, lensing changes the direction of the velocity of the light, but not the magnitude. The angle of deflection is:

$$\theta = \frac{4GM}{rc^2},$$

Where  $M$  is the mass at a distance  $r$  from the affected radiation,  $G$  is the universal constant of gravitation and  $c$  is the speed of light in a vacuum: the more the mass, the more the light angle deflection. In such a way, we are able to achieve the total quantity of matter which causes the gravitational lens effect: by measuring the distortion geometry, the mass of

the intervening cluster causing the phenomena can be obtained. In the case of the Universe, according to the Einstein's dictates, the 4D dimension (the spacetime) occurs when the mechanism of gravitational lensing takes place. It means that the fourth dimension "appears" just when the light is projected, through gravitational lensing, in a dimension higher, while the hidden galaxy is equipped with just three dimensions. Therefore, according to BUT and Einstein claims, the gravitational lensing lies in a  $R^n$  space, i.e., a 4D riemannian manifold (the spacetime), while the "hidden" celestial body, which generates the light producing the gravitational lens, needs to lie in a  $R^{n-1}$  space, i.e., the three "classical" Euclidean dimensions. This means that we achieve a dimensionality reduction: a Universe equipped with just three dimensions, plus the time. The latter is the fourth dimension, provided that we consider it as superimposed to a 3D Universe. Thus, we are allowed to argue that the angle reflection is caused by a further dimension, displayed by the n-sphere generated by the gravitational lens. Without such a higher dimension, the angle reflection does not exist and the mass cannot be measured.

**Gauge fields and time in the framework of BUT.** According to BUT, we achieved a system with three dimensions plus the time. In such a vein, what is the role of the time? We need to invoke once again BUT, and its close relationships with the symmetries. Symmetries are widespread invariances underlining countless physical and biological systems (Weyl)<sup>32</sup>. A symmetry break occurs when the symmetry is present at one level of observation, but "hidden" at another level (Roldán)<sup>33</sup>. BUT tells us that we can find, on an  $n$ -dimensional sphere, a pair of opposite points that have same encoding on an  $n-1$  sphere. This means that symmetries can be found when evaluating the system in a proper dimension, while they disappear (are hidden or broken) when we evaluate the same system in just one dimension lower. We emphasize that the symmetries are widespread at every level of organization and may be regarded as the most general feature of systems, perhaps more general than free-energy and entropy constraints too. Indeed, recent data suggest that thermodynamic requirements have close relationships with symmetries. The recent, interesting observation that entropy production is strictly correlated with symmetry breaking in quasistatic processes paves the way to use system invariances for the estimation of the free energy of metastable states and the energy requirements of computations and information processing (Roldán)<sup>33</sup>. Thus, giving insights into symmetries provides a very general approach to every kind of systems function. In such a vein, BUT provides a topological methodology for the evaluation of the most general features of systems activity, i.e., the symmetries, cast in a physical fashion that has the potential to be operationalized. The symmetries, in turn, are closely linked with gauge theories, and in particular with gauge fields. The n-sphere displaying the antipodal points (the symmetries) is equipped with a dimension more than the euclidean space where the the single point (symmetry break) occurs. This extra-dimension where BUT occurs might stand for a gauge field which, superimposed to the system, gives rise to the invariance of the symmetry, by "restoring" it with the simple add of a unity to the  $n$  member of BUT (from  $R^n$  to  $R^{n+1}$ ). Although BUT was originally limited to the case of  $n$  being a natural number which expresses a structure embedded in a spatial dimension, nevertheless the value of  $n$  in the brain  $S^n$  can also stand for other types of numbers (Tozzi)<sup>27</sup>. The  $n$  exponent does not need necessarily either to be a natural number or embedded in a spatial dimension. The  $n$  value of  $S^n$  can be casted as an integer, a rational or an irrational number. The BUT can be used not just for the description of "spatial" dimensions equipped with natural numbers, but also of antipodal points on spheres equipped with other kinds of  $n$ 's dimensions, for example a fractal dimension  $d$ . It allows us to use the  $n$  parameter as a versatile tool for the description of systems symmetries.

## CONCLUSION

We showed that the vector of time is able to represent the energetic gradient of the system, locally "broken" by timeless perturbations. We also provided a topological approach to gravitational lensing which strengthens our hypothesis. It allows us to draw some conclusions.

In analytical mechanics, the concept of virtual displacement - related to virtual work - is meaningful only when discussing a system subject to constraints on its motion. As stated above, this is the case of physical and biological activity. Virtual displacements occur exclusively in space and the underrated role of the sole "spatial" modifications needs to be emphasized when bearing in mind physical and biological activities. While virtual displacements take place, time is fixed and  $\delta t = 0$ . Thus, changes in physical/biological functions can be independent of the passage of time. When time equals  $= 0$ , the real trajectory does not exist: it is the passing of time that gives rise to the real displacement. It has been recently suggested that time is an emergent phenomenon arising from the quantistic entanglement and it exists just for observers inside the universe<sup>25</sup>: any god-like observer outside sees a static, unchanging universe, just as the Wheeler-DeWitt equations predict (note that time plays a role neither in such equations, nor in the formulation of the entangled states). If time stands for a continuous gauge field acting on the system's Universe, the theory of a 4D Riemannian Universe needs to be revised: time is not anymore one of the four coordinates of the phase space of the system Universe, but becomes just a field, a vector superimposed to an otherwise "simple" 3D Universe. It may also be hypothesized that the virtual constraints in the Universe stand for singularities and timeless perturbations, which could be regarded as places in which life occurs.

## REFERENCES

1. Kravchick, D.O. & Jordan, B.A. Presynapses go nuclear! *EMBO J.* **34**, 984-986 (2015).
2. Linkenkaer-Hansen, K., Nikouline, V.V., Palva, J.M., & Ilmoniemi R.J. Long-range temporal correlations and scaling behavior in human brain oscillations. *J. Neurosci.* **21**, 1370-1377 (2001).
3. Papo, D. How can we study reasoning in the brain? *Front Hum Neurosci.* **9**, 222 (2015).
4. Ribault, C., Sekimoto, K. & Triller, A. From the stochasticity of molecular processes to the variability of synaptic transmission. *Nat. Rev. Neurosci.* **12**, 375–387 (2011).
5. Bryngelson, J.D. & Wolynes, P.G. Spin glasses and the statistical mechanics of protein folding. *Proc. Natl. Acad. Sci. U S A.* **84**, 7524-7528 (1987).
6. Ferreiro, D.U, Hegler, J.A., Komives E.A. & Wolynes, P.G. On the role of frustration in the energy landscapes of allosteric proteins. *Proc Natl Acad Sci U S A.* **108**, 3499-503 (2011).
7. Onuchic, J.N., Luthey-Schulten, Z. & Wolynes, P.G. Theory of protein folding: the energy landscape perspective. *Annu. Rev. Phys Chem.* **48**, 545-600 (1997).
8. Sutto, L., Lätzer, J., Hegler, J.A., Ferreiro, D.U., & Wolynes, P.G. Consequences of localized frustration for the folding mechanism of the IM7 protein. *Proc. Natl. Acad. Sci. U S A.* 2007 **104**, 19825-19830 (2007).
9. Torby, B. *Energy Methods. Advanced Dynamics for Engineers.* HRW Series in Mechanical Engineering (CBS College Publishing, United States of America, 1984).
10. Goldstein, H. *Classical Mechanics* (Addison-Wesley Publishing Co., Reading, Massachusetts, 1980).
11. Sommerfeld, A. *Mechanics, Lectures on Theoretical Physics, vol. I* (Academic Press, New York, 1952).
12. Landau, L.L. & Lifshitz, M. *Mechanics* (Pergamon Press, Oxford, 1976).
13. Canudas-de-Wit, C. On the concept of virtual constraints as a tool for walking robot control and balancing. *Annual Reviews in Control* **28**, 157–166 (2004).
14. Stepp, C.E., Hillman, R.E. & Heaton, J.T. A virtual trajectory model predicts differences in vocal fold kinematics in individuals with vocal hyperfunction. *J Acoust Soc Am.* **127**, 3166-3176 (2010).
15. Kolar, I. & Michor, P. W. *Natural operations in differential geometry* (Springer-Verlag, Berlin, 1993).
16. Abraham, R.H. & Marsden, J. E. *Foundations of mechanics*, (Benjamin-Cummings, London, 1978).
17. Lang, S. *Differential and Riemannian manifolds* (Springer-Verlag, Berlin, New York, 1995).
18. Van Essen, D.C. A Population-Average, Landmark- and Surface-based (PALS) atlas of human cerebral cortex. *Neuroimage* **28**, 635–666 (2005).
19. Ehresmann, C. Les connexions infinitésimales dans un espace fibrée différentiable. *Colloque de Topologie, Bruxelles*, pp. 29–55 (1950).
20. DeWitt, B.S. Quantum Theory of Gravity II. The Manifestly Covariant Theory. *Phys. Rev.* **160**, 1195-1239 (1967).
21. Higgs, P.W. Broken Symmetries and the Masses of Gauge Bosons. *Phys. Rev. Lett.* **13**, 508 (1964).
22. 't Hooft, G. Renormalizable Lagrangians for massive Yang-Mills fields. *Nuclear Physics B* **35**, 167–188 (1971).
23. Zeidler, E. *Quantum Field Theory III: Gauge Theory.* Springer-Verlag, Berlin, Heideberg (2011).
24. Helland, I. S. Statistical inference under symmetry. *International Statistical Review* **72**, 409-422 (2004).
25. Moreva, E.V., Brida, G., Gramegna, M., Giovannetti, V., Maccone, L. & Genovese, M. Time from quantum entanglement: An experimental illustration. *Physical Review A* **89**, 052122 (2013).
26. De Wit, C.C., P. Tsiotras, E. Velenis, M. Basset, G. Gissing, Dynamic tire friction models for vehicle traction/braking control, *Vehicle System Dynamics* 39(3),189-226 (2003).
27. Tozzi A., Peters J.F. A topological approach unveils system invariances and broken symmetries in the brain. *Journal of Neuroscience Research*, 2016, in press.
28. Peters, J.F. *Computational Proximity. Excursions in the Topology of Digital Images*, Springer, 2016, in press.
29. Borsuk, K. Drie satze uber die n-dimensional euklidische sphere, *Fund. Math.* **XX**, 177-190 (1933).
30. Borsuk, K. Concerning the classification of topological spaces from the standpoint of the theory of retracts, *Fund. Math.*, **XLVI**, 321-330 (1959), MR0104216.
31. Dodson, C.T.J., Parker, P.E. *A user's guide to algebraic topology*, Kluwer, 1997, xii+405 pp., MR1430097.
32. Weyl, H (1982). *Symmetry*. Princeton: Princeton University Press. ISBN 0-691-02374-3.
33. Roldán E, Martínez IA, Parrondo JMR, Petrov D. Universal features in the energetics of symmetry breaking. *Nature Physics* **10**, 457–461 (2014) doi:10.1038/nphys2940